Directed Evolution of the α-L-Fucosidase from *Thermotoga maritima* into an α-L-Transfucosidase†

George Osanjo,‡ Michel Dion, Jullien Drone, Claude Solleux, Vinh Tran, Claude Rabiller, and Charles Tellier*

Université de Nantes, Nantes Atlantique Universités, UMR CNRS 6204, Biotechnologie, Biocatalyse, Biorégulation, Faculté des Sciences et des Techniques, 2, rue de la Houssinière, BP 92208, Nantes, F- 44322 France

Received July 17, 2006; Revised Manuscript Received November 15, 2006

ABSTRACT: The α-L-fucosidase from *Thermotoga maritima* (Tmαfuc) was converted into α-L-transfucosidase variants by directed evolution. The wild-type enzyme catalyzes oligosaccharide synthesis by transfer of a fucosyl residue from a *p*NP-fucoside donor to *p*NP-fucoside (self-condensation) with α-(1→3) regioselectivity or *p*NP-galactoside (transglycosylation) with α-(1→2) regioselectivity at low yields (7%). The wild-type enzyme was submitted to one cycle of mutagenesis, followed by rational recombinaton of the selected mutations, which allowed identification of variants with improved transferase activity. The transferase and hydrolytic kinetics of all the mutants were assessed by NMR methods and capillary electrophoresis. It was shown that the best mutant exhibited a dramatic 32-fold increase in the transferase/hydrolytic kinetic ratio, while keeping 60% of the overall wild-type enzyme activity. Accordingly, the maximum yield of a specific transglycosylation product [*p*NP-Gal-α-(1→2)-Fuc] reached more than 60% compared to 7% with WT enzyme at equimolar and low concentrations of donor and acceptor (10 mM). Such an improvement was obtained with only three mutations (T264A, Y267F, L322P), which were all located in the second amino acid shell of the fucosidase active site. Molecular modeling suggested that some of these mutations (T264A, Y267F) cause a reorientation of the amino acids that are in direct contact with the substrates, resulting in a better docking energy. Such mutants with high transglycosidase activity may constitute novel enzymatic tools for the synthesis of fucooligosaccharides.

α-L-Fucosidases (EC 3.2.1.51) are exoglycosidases capable of cleaving terminal α-L-fucosyl residues from glycoconjugates involved in a variety of biological processes, such as inflammation, tumor metastasis, fertilization, and the genetic disease fucosidosis (*1*, *2*). Indeed, L-fucose is one of the most common monosaccharides occurring at the nonreducing end of many glycans on mammalian cell surfaces, blood group antigens, and human milk oligosaccharides (*3*, *4*). Fucose-containing glycans are involved in a number of critical infectious and inflammatory diseases (*5*). For example, the H-type blood group antigens, which occur on enteroepithelial glycoproteins, have recently been shown to serve as receptors for noroviruses, the leading etiologic agents for viral diarrhea in children (*6*, *7*). Ruiz-Palacios et al. (2003) have shown that fucosyl oligosaccharides found in milk inhibit the colonization of human intestinal mucosal cells by *Campylobacter jejuni*, a well-known enteropathogen (*8*).

Despite their involvement in critical biological roles, fucooligosaccharides remain relatively inaccessible to scientific and pharmaceutical research due to the difficulties inherent in their synthesis. Significant advances have been made in chemical oligosaccharide synthesis (*9*). Nonetheless, synthesis on a cost-effective scale still remains a major obstacle. For instance, commercially available fucosyllactose is currently extracted from human milk. Using this source is complicated by the possibility of contamination by human pathogens.

The enzymatic synthesis of fucooligosaccharides is an alternative to chemical methods (*10*). Two types of enzyme can carry out fucosylation. The first group includes fucosyl transferases, which exhibit high specificity toward the acceptor and do not hydrolyze the product (*11*). However, these are often difficult to purify due to their association with membranes. Moreover, they require fucosyl nucleotide (GDP-fuc), which is not readily available, and need a complex multienzymatic system to be regenerated. As an alternative, fucooligosaccharides have been produced in vivo at low scale by engineering bacterial strains (*12*, *13*).

The other alternative for the synthesis of fucosyl glycans is to exploit the transfer activity of α-L-fucosidases. These enzymes are widely distributed in living organisms, being found in bacteria (*14*, *15*), fungi (*16*), plants (*17*), and mammals (*18*−*20*). On the basis of their amino acid sequence similarities, all α-L-fucosidases have been classified in a particular family (CAZy GH-29) (*21*).[1] However, information concerning their reaction mechanism has only recently become available and suggests that these enzymes hydrolyze fucosyl derivatives with retention of the anomeric configu-

† This work was supported by a grant from the French Embassy in Nairobi (Kenya) to G.O. and from the Region Pays de la Loire, France (VANAM program).

* To whom correspondence should be addressed. Phone: 33 (0)2 51 12 57 33. Fax: 33 (0)2 51 12 56 37. E-mail: Charles.Tellier@univ-nantes.fr.

‡ Present address: Department of Biochemistry, University of Nairobi (Kenya).

[1] Available at afmb.cnrs-mrs.fr/CAZY.

10.1021/bi061444w CCC: $37.00
Published on Web 12/30/2006

ration, an aspartyl residue being used as the catalytic nucleophile (*22*, *23*). Accordingly, some of the best characterized α-L-fucosidases have been shown to exhibit transglycosylation properties (*19*), a property which is only possible with a double displacement mechanism.

The transglycosylation activity of α-L-fucosidases is highly variable depending on the origin of the enzymes (*18*) but suggests that these enzymes may be attractive for synthesizing fucosylated oligosaccharides. However, they usually catalyze the hydrolysis of glycoside bonds while oligosaccharide yields remain generally moderate. Moreover, even when high regioselective preferences have been exerted by glycosidases, the presence of undesired regioisomers, which make the purification step difficult, has encouraged researchers to improve the properties of glycosidases by different strategies.

We have previously demonstrated that directed evolution can produce *Bacillus* α-galactosidase mutants displaying completely new regioselectivities while keeping their transglycosylation abilities (*24*, *25*). More recently, directed evolution has been applied to the *β*-glycosidase of *Thermus thermophilus* (Tt*β*-Gly) in order to obtain mutants with increased transglycosylation power (*26*). Using a simple screening procedure, we could produce mutant enzymes having a very high transfer activity. In one step of random mutagenesis and screening, followed by rational recombination of the selected mutations, the hydrolysis of substrates and of transglycosylation products was considerably reduced. We have shown that the properties of these new transglycosidases can compete with those of a glycosynthase mutant (*27*) while using more stable and commercially available donor substrates.

Here, we have extended this directed evolution approach to α-L-fucosidase from *Thermotoga maritima* (Tmαfuc) in order to obtain a mutant with high transfucosidase activity. This strategy looked particularly interesting for α-glycosidases because the alternative glycosynthase strategy, based on the mutation of the nucleophilic residue and the use of a *β*-glycosyl fluoride as the donor substrate (*28*, *29*), is limited by the poor stability of the *β*-glycosyl fluoride donor. Hydrolysis of *β*-glycosyl fluoride is thought to compete with the transglycosylation reaction, especially at high temperature, leading to low synthetic yields (*30*). Furthermore, efforts to develop α-fucosynthases using α-fucosides and external nucleophiles such as formate (*23*, *31*) have not yet borne fruit, hence the need to provide alternative effective enzymes.

We have demonstrated that the transglycosylation capacity of thermostable α-L-fucosidase (*32*) from the hyperthermophile *T. maritima* can be dramatically improved using a specific screening strategy after subjecting the enzyme to in vitro evolution.

MATERIALS AND METHODS

Materials. Enzyme substrates were purchased from Sigma, unless otherwise stated. Synthetic primers were made by Sigma Genosys. *T. maritima* genomic DNA was the generous gift of Dr. Laetitia Guevel.

Cloning. The gene TM0306 of *T. maritima* that encodes an α-L-fucosidase was amplified by PCR[2] from genomic DNA using the primers Fuc1 (5′-ATATGACATATGATTTC-TATGAAACCCCG-3′) and Fuc2 (5′-GATAACAAGCTT-TCATTCTTCCACCGCCTCCAAC-3′), which carry the *Nde*I and *Hin*dIII restriction, sites, respectively. The sequences recognized by the enzymes are underlined.

Twenty picomoles of each primer was mixed with 50 ng of genomic DNA in a 50 *μ*L PCR. The reaction conditions were 1× *Pfu* buffer, 0.2 mM each dNTP, and 2.5 units of *Pfu* DNA polymerase. The reaction mixture was thermocycled for 5 min at 94 °C and then for 30 cycles at 94 °C for 1 min, 50 °C for 30 s, and at 72 °C for 5 min. The PCR product was digested by *Nde*I and *Hin*dIII restriction enzymes and cloned into the pET21a vector (Novagen) digested by the same enzymes. The resulting plasmid was termed pET21Fuc. The expression of the ORF TM0306 in this plasmid is under the control of the T7 RNA polymerase promoter inducible by isopropyl 1-thio-*β*-D-galactopyranoside (IPTG). The plasmid pET21Fuc was used to transform *Escherichia coli* Novablue cells (Novagen), which were plated on LB agar plates containing 100 *μ*g/mL ampicillin and 0.1 mM X-Fuc. After overnight growth, clones expressing α-L-fucosidase activity turned blue.

Random Mutagenesis. Random mutations were introduced by mutagenic PCR (*33*). Primers T_7P (5′-TTAATACGACT-CACTATAGC-3′) and T_7T (5′-GCTAGTTATTGCTCAGCG-GC-3′) flank the gene before the *Ptac* promoter and after the *Hin*dIII restriction site. Twenty picomoles of each primer was mixed with 50 ng of the plasmid pET21Fuc in a 50 *μ*L PCR. The reaction conditions were 1× *Taq* buffer, 1 mM dTTP and dCTP, 0.2 mM dATP and dGTP, 7 mM $MgCl_2$, and 2.5 units of *Taq* DNA polymerase (Goldstar). The reaction was thermocycled as follows: one cycle at 94 °C for 5 min and then 30 cycles at 94 °C for 30 s, 50 °C for 30 s, and 72 °C for 2 min 30 s. Mutagenized PCR products were digested by the *Nde*I and *Hin*dIII restriction enzymes and cloned back into the pET21a vector digested by the same enzymes.

Introduction of a His Tag. The primers FucB1 (5′-T A T A T A G A A T T C A T G C A C C A C C A C C A C C A C-CACCACCATATGATTTCTATGAAACCCCGTTAC-3′), incorporating a His_6 codon and an *Eco*RI site, and Fuc2 (sequence given above) were used to amplify the genes encoding the wild-type enzyme and selected mutants. The polymerase DyNazyme (Finnzyme) in its buffer was used to achieve amplification in the standard reaction conditions. The PCR products were digested by *Eco*RI and *Hin*dIII restriction enzymes and cloned into the plasmid pBTac2 digested by the same enzymes. The expression vector containing the ORF TM0306 that encodes *Tmαfuc* under the control of the *Ptac* promoter was termed pBFuc. *E. coli* XL1 blue MRF′ was used to express the enzymes cloned in pBTac2.

Screening of Mutants. The plasmid pBFuc carrying mutagenized *Tmαfuc* genes was used to transform *E. coli* XL1 blue cells. After overnight growth on LB agar impregnated

[2] Abbreviations: WT, wild type; X-Fuc, 5-bromo-4-chloro-3-indolyl α-L-fucopyranoside; *p*NP, *p*-nitrophenyl; PCR, polymerase chain reaction; NMR, nuclear magnetic resonance; COSY, correlated spectroscopy.

with X-Fuc (0.1 mM), colonies expressing the wild-type *Tmαfuc* gene gave dark blue spots (88%) even at 37 °C, while mutants expressing inactive fucosidase or *E. coli* clones carrying empty inserts gave white colonies (3%). Transformed *E. coli* cells that expressed fucosidase with low hydrolytic activity gave pale blue colonies (9%). These colonies were selected and cultivated, and their transglycosylation activity was screened as follows: 3 mL of an overnight LB medium culture of the selected clones was centrifuged and the cell pellet suspended in 200 μL of 50 mM citrate−phosphate buffer, pH 5.5, containing 145 mM NaCl. After brief sonication, the cell lysate was centrifuged and enzyme activity in the supernatant determined. One unit of enzyme was introduced into a reaction mixture containing 25 mM *p*NP-αFuc (donor) with or without 50 mM acceptor [*p*NP-*β*Gal or phenyl lactobiose [*β*-D-Gal(1→3)-*β*-D-Glc-O-phenyl]] in 145 mM NaCl and 50 mM citrate−phosphate buffer, pH 5.5, containing 5% dimethyl sulfoxide (DMSO) and incubated at 60 °C. Aliquots of 2 μL were withdrawn and monitored by TLC (chloroform/methanol/water/acetic acid, 28:10:2:1).

Rational Recombination of Mutants. Mutations giving beneficial effects were recombined with the aid of the restriction endonucleases *Eag*I and *Acc*I, which cut in the middle of the *Tmαfuc* gene. As an example, to obtain the double mutant T264A/L322P, the full-length genes containing each of the mutations were incubated with *Eag*I. *Eag*I digested the DNA sequence only at the level of codon 264 but did not disrupt the mutation. The DNA fragments were purified and ligated after swapping the fragments encoding the two mutations. The product of recombination was subsequently ligated onto the plasmid vector. A similar procedure was performed to generate the triple and quadruple mutants. The success of the method was confirmed by sequencing.

Protein Purification. To prepare His-tagged enzymes, *E. coli* XL1 blue MRF′ carrying the vector pBFuc was cultivated in 200 mL of LB medium at 37 °C for 18 h without induction. The cells were harvested by centrifugation for 10 min at 10000*g* and suspended in suspension buffer (50 mM NaH_2PO_4, pH 8.0, 300 mM NaCl, 10 mM imidazole) and lysed by incubating for 1 h after addition of lysozyme (0.2 mg/mL) followed by sonication. Thermolabile proteins were precipitated by heating at 70 °C for 30 min. The cell debris was removed by centrifugation as described above. The His-tagged enzymes in the supernatant were purified by Ni^{2+}-affinity chromatography using the QIAexpressionist protein purification kit (Qiagen).

Enzyme Kinetics. Kinetic studies at 40 °C were performed with purified enzymes on chromogenic substrates (*p*NP-αFuc) in microtitration plates by following continuous changes in absorbance at 405 nm using a microplate reader (iEMS; Labsystem). Reaction mixtures (190 μL), containing the substrate (concentration range from 0.01 to 5 mM) and buffer (50 mM citrate−phosphate, 140 mM NaCl, pH 5.5), were preincubated in the plate holder for 10 min prior to addition of 10 μL of enzyme solution. Kinetic studies at 70 °C were performed in 50 mM citrate−phosphate and 140 mM NaCl, pH 5. The 4-nitrophenol released was measured at 405 nm using 100 μL aliquots of the reaction solution diluted with 100 μL of 1 M iced sodium carbonate. The molar extinction coefficient of 4-nitrophenol was determined for each experimental condition using a calibration curve established from 4-nitrophenol concentrations. The kinetic parameters k_{cat} and K_m were calculated by fitting the initial rate data to the Michaelis−Menten equation using Origin7 (OriginLab). One unit of activity is defined as the amount of enzyme that liberates 1 μmol of *p*-nitrophenol/min under the given assay conditions.

Capillary Electrophoresis. For kinetic studies of transglycosylation by capillary electrophoresis, 1 unit of enzyme was introduced into reaction mixtures containing 10 mM *p*NP-αFuc (donor) with or without 10 mM acceptor (*p*NP-*β*Gal) in 50 mM sodium citrate and phosphate buffer and 145 mM NaCl, pH 5 at 40 °C. Aliquots of 5 μL were withdrawn at different times and mixed with 40 μL of 50 mM Borax buffer, pH 9.15. *p*NPAcetate (5 μL, 2.5 mM) was added as an internal standard. Separation of the reaction products was performed using a Beckman P/ACE System 5000 with an uncoated fused-silica capillary 54 cm long with an internal capillary diameter of 120 μm. Separation was done in the electroendoosmotic mode under the following conditions: voltage, 15 kV (80 μA); injection pressure, 0.5 psi from cathode; running buffer, 50 mM Borax buffer, pH 9.15. Products were detected and quantified by UV absorbance at 214 nm. Between runs, the capillary was rinsed for 2 min with 100 mM NaOH followed by water for 2 min and then with 50 mM Borax buffer, pH 9.15, for 2 min. Initial velocities of the transglycosylation reactions were determined from the amount of *p*NP α-L-Fuc*p*-(1→3)-α-L-Fuc*p* and *p*NP α-L-Fuc*p*-(1→2)-*β*-D-Gal*p* synthesized as a function of time using the integration software of the Beckman P/ACE System 5000. The rates of hydrolysis were calculated from the difference between the overall activity, determined from the amount of 4-nitrophenol liberated over the reaction course, and the transglycosylation rate.

NMR Spectroscopy. NMR spectra were recorded with either Bruker AX400 or DRX500 spectrometers using D_2O or D_2O buffer solutions as solvent. In all cases, chemical shifts, in parts per million, were quoted from the resonance of methyl protons of sodium 3-(trimethylsilyl)propanesulfonate as an internal reference.

Determination of Yields. The yields were determined by means of experiments performed directly in the NMR tube maintained at 65 °C in the spectrometer. ^1H NMR spectra were recorded every 15 min until complete consumption of the donor (*p*NP-Fuc) occurred. Yields were calculated from the integration of characteristic proton signals of each component at maximal concentration of transglycosylation products. The percentage value for each compound was expressed as a fraction of donor (*p*NP-αFuc) using the equations:

$$\%\ \text{condensation saccharide } i^C = \frac{I_i^C}{\sum_i^j I_i^C + 2\sum_i^j I_i^S}$$

$$\%\ \text{condensation saccharide } i^S = \frac{2I_i^S}{\sum_i^j I_i^C + 2\sum_i^j I_i^S}$$

where i^S represents a self-condensation transglycosylation reaction product and i^C a transglycosylation product, the remaining *p*NP-αFuc or L-fucose. I_i^S is the integration value for the resonance signal of one proton of a product i^S, and I_i^C is the same integration value for a product i^C.

For the self-condensation reaction, *p*NP-αFuc (90 μmol, 150 mM) was dissolved in buffer A [600 μL of 100 mmol/L sodium phosphate buffer in D_2O (pD 5.0) containing DMSO-d_6 (10% v/v)]. For transglycosylation reactions with acceptor **1**, *p*NP-αFuc (donor, 12 μmol, 20 mM), and *p*NP-βGal as an acceptor **1**, 24 or 60 μmol (40 or 100 mM) was dissolved in buffer B (600 μL of 100 mM sodium phosphate buffer in D_2O, pD 5.0). For transglycosylation reactions with acceptor **2** (phenyl β-D-Gal*p*-(1→3)-β-D-Glc*p*), *p*NP-αFuc (donor, 30 μmol, 50 mM) and **2** (60 μmol, 100 mM) were dissolved in buffer A. Then, 5 μL of the native enzyme solution (5−10 μg of enzyme) was added.

pNP α-L-*Fucp*-(1→*3*)-α-L-*Fucp* (***3***). *p*NP-αFuc (15 mg, 52 μmol, 20 mM) was dissolved into 2.6 mL of buffer C (50 mM sodium citrate and phosphate, 145 mM NaCl, pH 5.0). Then, 40 μL of the native enzyme solution (80 μg of enzyme) was added, and the reaction mixture was stirred for 1 h at 60 °C. The resulting yellow solution was evaporated under reduced pressure, and the dry colorless residue was purified by silica gel chromatography ($CHCl_3$/MeOH/AcOH/H_2O, 85:30:3:5 v/v) to afford **3** (4 mg, 17%) as white foam. Small amounts of another nonidentified regioisomer (3%) and a trisaccharide (7%) were also present. NMR studies (Bruker instrument 400 MHz, ^1H, ^{13}C, COSY, and $^1H-^{13}C$ correlation) were conducted at 333 K in pyridine-d_5 using sodium 3-(trimethylsilyl)propanesulfonate as an internal reference standard.

^1H (^{13}C) NMR signal assignments: 6.096 H1I (J = 3.5 Hz) (99.8 C1I), 5.653 H1II (J = 3.5 Hz) (97.6 C1II), 4.886 H5I (J = 6.4 Hz) (67.9 C5I), 4.820 H2I (J = 9.4 Hz) (67.5 C2I), 4.655 H3I (J = 2.9 Hz) (77.3 C3I), 4.652 H2II (J = 9.4 Hz) (70.1 C2II), 4.544 H3II (J = 2.9 Hz) (71.7 C3II), 4.322 H4I (69.0 C4I), 4.208 H5II (J = 6.2 Hz) (68.2 C5II), 1.547 H6I (17.1 C6I), 1.511 H6II (16.9 C6II).

pNP α-L-*Fucp*-(1→*2*)-β-D-*Galp* (***4***) *and pNP* α-L-*Fucp*-(1→*6*)-β-D-*Galp* (***5***). *p*NP-αFuc (104 mg, 0.36 mmol, 18 mM) and *p*NP-βGal (600 mg, 2 mmol, 5.5 equiv) were dissolved into 20 mL of buffer C. Then, 100 μL of the native enzyme solution (200 μg of enzyme) was added, and the reaction mixture was stirred at 60 °C for 2 h. Next, 100 μL of native enzyme solution was added, and the reaction was allowed to proceed for a further 1 h. The resulting yellow solution was evaporated under reduced pressure, and the dry colorless residue was purified as follows. Silica gel chromatography (AcOEt/MeOH/H_2O, 7:2:1 v/v) of the latter residue afforded a partially enriched mixture of **4** and **5** (38 mg). This mixture was acetylated by treatment with a solution of Ac_2O/pyridine (10 mL, 1:1 v/v) at room temperature for 2 days. Evaporation under reduced pressure and flash chromatography (15% petroleum ether/diethyl ether) afforded the inseparable peracetylated mixture of **4** and **5** (44 mg). Final deprotection was achieved by treatment of peracetylated compounds with sodium methylate (5 mL, 20 mM in MeOH) at 4 °C for 1.5 h. The mixture was then neutralized by the addition of Amberlite resin IR-120 (H^+ form), filtrated, and evaporated under reduced pressure to afford a clean mixture of **4** and **5** (15 mg).

^1H (^{13}C) NMR signal assignments of **4**: 5.931 H1II (J = 3.9 Hz) (101.7 C1II), 5.703 H1I (J = 7.6 Hz) (104.6 C1I), 4.857 H2I (J = 9.4 Hz) (81.8 C2I), 4.744 H2II (J = 9.9 Hz) (72.1 C2II), 4.671 H4I (70.8 C4I), 4.600 H3II (J = 2.3 Hz) (72.9 C3II), 4.600 H5II (69.2 C5II), 4.600 H6I (J = 4.7 Hz) (63.4 C6I), 4.480 H6′I (J = 6.5 Hz) (63.4 C6I), 4.480 H3I (J = 2.9 Hz) (76.6 C3I), 4.256 H4II (74.5 C4II), 1.521 H6II (J = 5.8 Hz) (18.5 C6II).

Phenyl α-L-*Fucp*-(1→*2*)-β-D-*Galp*-(1→*3*)-β-D-*Glcp* (***6***). *p*NP-αFuc (142 mg, 0.50 mmol, 50 mM) and phenyl β-D-Gal*p*-(1→3)-β-D-Glc*p* (418 mg, 1 mmol, 2 equiv) were dissolved into 10 mL of buffer D [50 mmol/L sodium citrate and phosphate (pH 5.0) containing NaCl (145 mmol/L) and DMSO (10% v/v)]. Then, 1000 μL of the B3 mutant enzyme solution (2 mg of enzyme) prepared as described above was added, and the reaction mixture was stirred at 70 °C for 3.5 h. The resulting yellow solution was evaporated under reduced pressure, and the dry colorless residue was purified by silica gel chromatography (AcOEt/MeOH/H_2O, 7:2:1 v/v) to afford **6** (120 mg, 43%) as a white foam.

^1H (^{13}C) NMR signal assignments: 5.779 H1III (J = 3.4 Hz) (104.6 C1III), 5.659 H1II (J = 7.6 Hz) (105.7 C1II), 5.382 H1I (J = 7.7 Hz) (103.1 C1I), 4.899 H5III (70.5 C5III), 4.661 H2II (83 C2II), 4.430 H2I (J = 9.1 Hz), 4.304 H3I (J = 8.3 Hz) (90.3 C3I), 4.206 H5II (J = 4.9 and 1 Hz) (78.8 C5II), 4.138 H5I (J = 2.1, 5.2, and 9.5 Hz) (80.0 C5I), 4.091 H4III (J = 2.8 and 1 Hz) (74.9 C4III, 63.9 C6I, 63.7 C6II, 18.8 C6III).

Molecular Modeling. Three X-ray crystal structures of WT Tmαfuc are accessible in the PDB (1HL9, 1HL8, and 1ODU) with resolutions of 2.25, 2.4, and 2.8 Å, respectively. The former and the latter structures are complexes with ligands of the fucopyranoside type. In each set of data, there are two protein chains in the asymmetric unit (A and B). As no complete structures are available (two or three missing loops in each chain), the selected starting geometry was 1HL9-B, which has the highest resolution of crystal structure and the shortest missing segments (47−55 and 269−274). To ensure the integrity of the structure throughout the calculations, heavy atoms at each end of the experimentally determined amino acid segments were fixed (R7-P46, D56-H268, and L275-E448). All calculations were performed with the CFF91 force field (*34*). For the enzyme, the crystal structure of the native Tmαfuc cocrystallized with 2-deoxy-2-fluorofucose was used (1HL9). The modeled ligands were the possible transglycosylation products *p*NP α-L-Fuc*p*-(1→*x*)-α-L-Fuc*p* and *p*NP α-L-Fuc*p*-(1→*x*)-β-D-Gal*p*. To systematically analyze the regioselectivity, (1→2), (1→3), and (1→4) linkages were taken into account for both types of product. The (1→6) linkage was not selected due to its supplemental degree of freedom between six-membered rings. For the selected disaccharides, the main degrees of freedom are located on the glycosidic linkages; thus all disaccharide maps [Fuc*p*-(1→*x*)-α-L-Fuc*p* and Fuc*p*-(1→*x*)-β-D-Gal*p*] with x = 2, 3, or 4 were generated to evaluate their flexibility according to the semirelaxed protocol already described (*35*). The first molecular modeling stage consisted of locating the nonreducing substrate ring (fucopyranose) assumed to fill the most deeply buried subsite (−1) using the crystallographic coordinates of the fucose ring as template. This complex with monomeric product was then refined using an energy optimization. The best solution was kept for subsequent

Scheme 1: Transglycosylation Reactions Catalyzed by α-L-Fucosidase from *T. maritima*

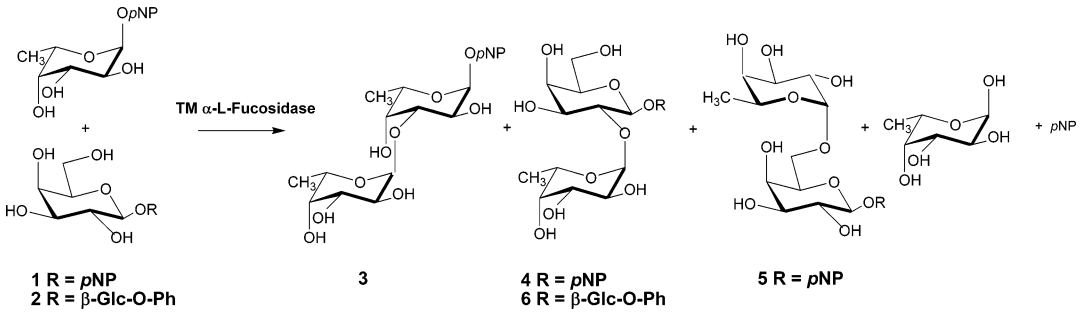

constructions by generating all possible conformations inside the catalytic site according to low-energy glycosidic junctions already determined for the six selected disaccharides. Complexes with steric conflicts between enzyme and product were discarded, and for all others, a series of energy minimizations were performed. At this stage, all sets of hydrogen bond networks were manually tested, and a geometrical criterion of an acceptable distance between the anomeric carbon and the nucleophilic residue D224 was kept throughout the minimization procedure. For mutated enzymes, only the best complex solutions for the WT enzyme were kept from which in silico mutations were performed, assuming a local arrangement in the vicinity of the replaced residue. Then, a full minimization procedure was carried out, and a complete reanalysis of hydrogen bond networks was done to refine these modified complexes. To compare all of these complex structures in terms of transglycosylation preferences, the global binding energy was calculated from these refined docking solutions. For more details, partial binding energies were also estimated for individual subsites in each case. The contribution of each subsite was estimated for product monomer and amino acid residues with at least one heavy atom <3.6 Å, a pyranose heavy atom. Hydrogen bonding and stacking terms were discriminated, and a van der Waals term was defined by subtraction from the total energy.

RESULTS

Regioselectivity of the Transfucosylation Reaction by the WT α-L-*Fucosidase.* Since no information was available concerning the transglycosylation activity and the regioselectivity of the reaction catalyzed by α-L-fucosidase from *T. maritima*, the course of the reactions using *p*NP-α-L-fucose as a substrate in the presence of various acceptors was monitored by means of in situ proton NMR spectroscopy (Scheme 1). When *p*NP-α-L-fucose was incubated with the WT Tmαfuc, the formation of L-fucose resulting from hydrolysis and self-condensation reaction products was observed (Table 1). The structure of the products, determined by standard NMR spectroscopy techniques (COSY, $^{1}H-^{13}C$ correlation) showed that Tmαfuc mainly produced *p*NP α-L-Fuc*p*-(1→3)-α-L-Fuc*p*, together with small amounts of another unknown regioisomer and trisaccharides. These results indicated that Tmαfuc has potentially good transglycosylation abilities, a property that is in accordance with the double inversion mechanism involving a glycosyl-enzyme intermediate (*22*).

To further assess the transglycosylation properties of Tmαfuc, various monosaccharides and disaccharides were tested as acceptors. The formation of transglycosylation products was assayed by TLC, NMR, and capillary electrophoresis. When *p*NP-*β*Gal was used as an acceptor, the main transglycosylation product was the disaccharide *p*NP α-L-Fuc*p*-(1→2)-*β*-D-Gal*p*. The yield of transglycosylation products, however, did not exceed 30% even at high acceptor concentrations. Surprisingly, the (1→2) regioselectivity observed during the condensation reaction was different from the (1→3) regioselectivity of the self-condensation reaction. This observation will be discussed later in this paper on the basis of molecular modeling studies. When a disaccharide [*β*-D-Gal-(1→3)-*β*-D-Glc-O-Ph] was used as acceptor, the corresponding trisaccharide was formed by transglycosylation in low yield due to the competing hydrolytic and self-condensation reactions (Table 1). However, the fucose unit was exclusively transferred on the galactosyl unit located at the nonreducing end.

It was apparent that the transglycosylation properties of WT Tmαfuc, while comparable to other known fucosidases (*15*, *18*), were not suitable for the synthesis of fucosylated oligosaccharides in high yields. So, we decided to use directed evolution procedures (*36*, *37*) in order to obtain mutants with improved transglycosylation properties.

Screening Procedure. In order to improve the transglycosylation/hydrolysis ratio of Tmαfuc, we first performed a random mutagenesis by error-prone PCR on the gene *Tmαfuc*. Amplification conditions were adjusted to generate mutations at the rate of 3−4 misincorporated base pairs per 1000 base pairs of the gene, resulting in a mean of 2 amino acid substitutions per fucosidase mutant. The screening of variants was carried out in two steps as previously described (*26*). First, mutants displaying lower hydrolytic activity than that of the wild-type enzyme were screened on LB plates containing X-Fuc (0.1 mM). At this low substrate concentration, far below the K_m for this substrate (1.4 ± 0.3 mM), we expected the self-condensation, which is dependent on substrate concentration, to be negligible. Consequently, pale blue colonies would express mutants with low hydrolytic activity. Then, among these mutants, we anticipated that some mutants would keep their transglycosylation activity in the presence of a suitable acceptor. With an activated donor substrate, such as X-Fuc or *p*NP-Fuc, the rate-limiting step in the double inversion mechanism is the deglycosylation; thus transglycosylation efficiency is dependent on the enzyme preference for an acceptor other than water. The mutants with improved transglycosylation capacity were selected by using TLC. The reaction products were obtained after incubation of the extracted mutant enzymes with *p*NP-Fuc as donor and *p*NP-Gal or phenyl lactobiose [*β*-D-Gal-(1→3)-*β*-D-Glc-O-phenyl] as acceptor.

Table 1: Transglycosylation Properties of WT Tmαfuc

donor	acceptor	donor/acceptor ratio	products	relative yield[a] (%)
*p*NP-αFuc	*p*NP-αFuc		fucose/**3**/X[b]/trisaccharide	19/17/3/7
*p*NP-αFuc	*p*NP-*β*Gal	1/2	fucose/**4**/**5**/**3**	70/14/7/8
*p*NP-αFuc	*p*NP-*β*Gal	1/5	fucose/**4**/**5**/**3**	63/23/8/traces
*p*NP-αFuc	*β*-Gal-(1−3)-*β*-Glc-O-Ph	1/2	fucose/**6**/Y[c]/**3**	65/8/4/19

[a] Molar percentages are the transient yield calculated at the time when transglycosylation is maximum and calculated from the integrations of the NMR signals of the various anomeric protons. [b] Undetermined disaccharide. [c] Undetermined trisaccharide.

Table 2: Mutations Found in Evolved Fucosidase Enzymes[a]

mutations	147	196	210	**226**	237	**264**	**267**	**322**
WT	R	P	M	**G**	Y	**T**	**Y**	**L**
Error-Prone PCR Mutants								
B3	G							**P**
B12						**A**		
B36		L			H		**F**	
Recombinants from Two Mutants								
C67						**A**		**P**
M3					H		**F**	**P**
N16			V		H	**A**		
R8			V		H	**A**	**F**	
Recombinants from Three Mutants								
P25				**S**	H	**A**		**P**
S1			V		H	**A**	**F**	**P**
C2						**A**	**F**	**P**
D2				**S**		**A**	**F**	**P**

[a] Amino acids in bold font are located in the second shell around the enzyme pocket.

About 5000 recombinant clones were screened according to this selection process. About 100 colonies displaying lower hydrolytic activity were chosen, and mutant enzymes were extracted and tested for transglycosylation reaction. The analysis of products by TLC revealed that three clones (B3, B12, B36) exhibited higher transglycosylation activity than that of the WT enzyme (data not shown).

Gene sequencing revealed that *Fuc*B12 had only one mutation at position 264 where the threonine residue of the WT enzyme was changed to alanine. *Fuc*B3 had two mutations, R147G and L322P, while *Fuc*B36 had three amino acid substitutions, P196L, Y237H, and Y267F (Table 2). Some mutations were located near the active site, like the T264A mutation in the B12 mutant or Y267F in the B36 mutant, but none of them was in direct contact with the substrate (*32*). Interestingly, mutation Y267F is located just after the acid/base residue E266 within the active site. Since these mutations were different for each mutant, we envisaged that a recombination of these mutants could possibly enhance the transglycosylation activity by a cumulative effect.

Rational Recombination of the Best Mutations. Taking into account the low number of mutants with improved transglycosylation activity and the fact that the number of mutations in each mutant did not exceed three, we constructed by site-directed mutagenesis most of the single mutants to identify the mutations that have a positive effect on transglycosylation activity.

First, it was noticed that the R147G substitution in mutant B3 did not alter the transglycosylation activity based on the TLC profile of the reaction products obtained after incubation of this mutant with *p*NP-αFuc and *p*NP-*β*Gal. This observation was expected since this mutation was located far from the active site at the surface of the enzyme structure. The effect of the P196L mutation in mutant B36 was deduced by comparison of the activities of the mutant B36 (P196L/Y237H/Y267F) and of the double mutant P5 (Y237H/Y267F). It appeared that this mutation was responsible for the lack of the regioselectivity of the B36 mutant since the double mutant P5 gave only α-L-Fuc*p*-(1→3)-α-L-Fuc*p* and *p*NP α-L-Fuc*p*-(1→2)-*β*-D-Gal*p* transglycosylation products while an additional regioisomer was obtained with B36. All other mutations, Y237H, T264A, Y267F, and L322P, which seemed, based on the qualitative screening process by TLC, to have an effect on the level of transglycosylation were kept to be rationally recombined.

Having determined potential positive mutations, rational combinations were made, first between two of the first generation mutants to create the recombinants: C67 (T264A/L322P), M3 (Y237H/Y267F/L322P), N16 (*M210V*/Y237H/T264A), and R8 (*M210V*/Y237H/T264A/Y267F). Then, recombinations of various potential positive mutations from all three initial mutants generated the mutants P25 (*G226S*/Y237H/T264A/L322P), S1 (*M210V*/Y237H/T264A/Y267F/L322P), C2 (T264A/Y267F/L322P), and D2 (*G226S*/T264A/Y267F/L322P) (Table 2). During the construction of mutants, additional mutations (*M210V* and *G226S*) occurred inadvertently, which necessitated the construction of the additional mutants S1 and D2 in order to determine the effect of these mutations (see below).

Kinetic Analysis of the Mutants. To quantify the effect of the mutations, the reaction kinetics of the improved mutants were studied on purified enzymes. After overexpression of the gene in *E. coli* with a His tag at the N-terminal end, the crude extracts were first heated for 30 min at 70 °C to eliminate most of the thermolabile proteins of *E. coli*. Then, pure Tmαfuc mutants were obtained following affinity chromatography on Ni-NTA resin. The steady-state kinetics of enzymatic reactions were first determined at 40 and 70 °C with *p*NP-Fuc as substrate (Table 3). Surprisingly, mutants from the first round of mutagenesis exhibited higher k_{cat} than the wild-type enzyme but a higher K_m, which was not expected for mutants selected for their low hydrolytic activity on X-Fuc.

To get quantitative information about both transglycosylation and hydrolysis activities, the kinetics of the reactions were followed directly by capillary electrophoresis using *p*NP-αFuc as donor (10 mM) and *p*NP-*β*Gal as acceptor (10 mM). The overall activity (hydrolysis plus transglycosylation) was determined by following the initial reaction rate of the release of free *p*-nitrophenol, while the kinetics of the formation of all the transglycosylation products [*p*NP α-L-Fuc*p*-(1→3)-α-L-Fuc*p* and *p*NP α-L-Fuc*p*-(1→2)-*β*-D-Gal*p*] were followed separately (Figure 1). Hydrolytic activity was deduced from the difference between the overall activity and the transglycosylation activity (Table 4). The mutants obtained after the first step of random mutagenesis, B3, B12, and B36, had a transglycosylation/hydrolysis (T/H) rate ratio about 10-fold higher than the wild-type enzyme, which demonstrated the validity and the efficiency of the screening process designed to select for mutants with improved transglycosylation activity. After recombination of the posi-

Table 3: Kinetic Parameters of WT and Mutant α-L-Fucosidase Enzymes at 40 °C and pH 5.5 and at 70 °C and pH 5 with *p*NP-αFuc as Substrate[a]

mutant	temp (°C)	k_{cat} (s^{-1})	K_m (mM)	k_{cat}/K_m (M^{-1} s^{-1})
WT	40	5.1 ± 0.2	0.020 ± 0.003	2.6×10^5
	70	35 ± 1	0.079 ± 0.007	4.4×10^5
B3	40	15 ± 0.5	0.13 ± 0.01	1.2×10^5
	70	198 ± 11	0.28 ± 0.03	7.1×10^5
B12	40	15 ± 0.4	0.065 ± 0.006	2.3×10^5
	70	169 ± 18	0.07 ± 0.01	2.5×10^6
B36	40	15 ± 0.8	0.09 ± 0.01	1.7×10^5
	70	164 ± 4	0.10 ± 0.01	1.6×10^6
C67	40	3.6 ± 0.1	0.19 ± 0.02	1.9×10^4
	70	50 ± 4	0.25 ± 0.06	2.0×10^5
M3	40	14.8 ± 0.6	0.29 ± 0.05	5.1×10^4
	70	96 ± 9	0.23 ± 0.04	4.2×10^5
N16	40	20 ± 0.5	0.10 ± 0.01	2.0×10^5
	70	65 ± 5	0.06 ± 0.01	1.1×10^6
R8	40	4.3 ± 0.1	0.09 ± 0.01	4.7×10^4
	70	56 ± 4	0.14 ± 0.02	4.0×10^5
P25	40	2.7 ± 0.1	0.08 ± 0.01	3.3×10^4
	70	39 ± 1	0.10 ± 0.01	3.9×10^5
S1	40	0.73 ± 0.02	0.14 ± 0.01	5.2×10^3
	70	20 ± 0.7	0.25 ± 0.02	8.0×10^4
C2	40	0.50 ± 0.06	0.06 ± 0.01	8.3×10^3
	70	8.2 ± 0.4	0.31 ± 0.04	2.7×10^4
D2	40	0.48 ± 0.01	0.09 ± 0.01	5.3×10^3
	70	6.4 ± 0.5	0.30 ± 0.06	2.1×10^4

[a] Kinetic constants were determined from the time-dependent release of *p*-nitrophenol at 405 nm.

tive mutations, an additional improvement in the T/H activity ratio was obtained, which led to a 30-fold overall increase of the T/H ratio. Interestingly, the evolution process did not affect the overall activity very much, since the decrease in the hydrolytic activity was partially compensated for by an increase in the transglycosylation activity for most of the mutants. The error-prone PCR mutants (B3, B12, and B36) exhibited a higher overall activity than that of the WT enzyme, which correlated to the higher observed k_{cat} (Table 3). However, these mutants had a higher K_m than the WT enzyme, particularly at low temperature, which led to a lower specificity constant (k_{cat}/K_m). These results are consistent with the screening process, carried out at low substrate concentration of X-Fuc, which selected colonies expressing mutants with a low k_{cat}/K_m for hydrolysis.

On the basis of the quantitative evaluation of the kinetic properties of the mutants C67 (T264A/L322P) and P25 (*G226S*/Y237H/T264A/L322P), which had similar kinetic properties (Table 4), it appeared that mutations Y237H and G226S did not significantly modify the transglycosylation properties of Tmαfuc. This observation was consistent with the localization of residue 237 at the surface of the Tmαfuc three-dimensional structure, far away from the substrate pocket (*32*). The neutral effect of the mutation G226S, which appeared as a mutational error during cloning of the mutant P25, was confirmed by the kinetic comparisons of mutants C2 (T264A/Y267F/L322P) and D2 (*G226S*/T264A/Y267F/L322P). The mutation *M210V*, which also appeared during the cloning process, did not have a significant effect on the transglycosylation properties since mutants S1 (*M210V*/Y237H/T264A/Y267F/L322P) and C2 (T264A/Y267F/L322P) showed similar V_{trans}/V_{hyd} ratios. However, this mutation could affect the overall activity of the mutant (Tables 3 and 4). The remaining three potential positive

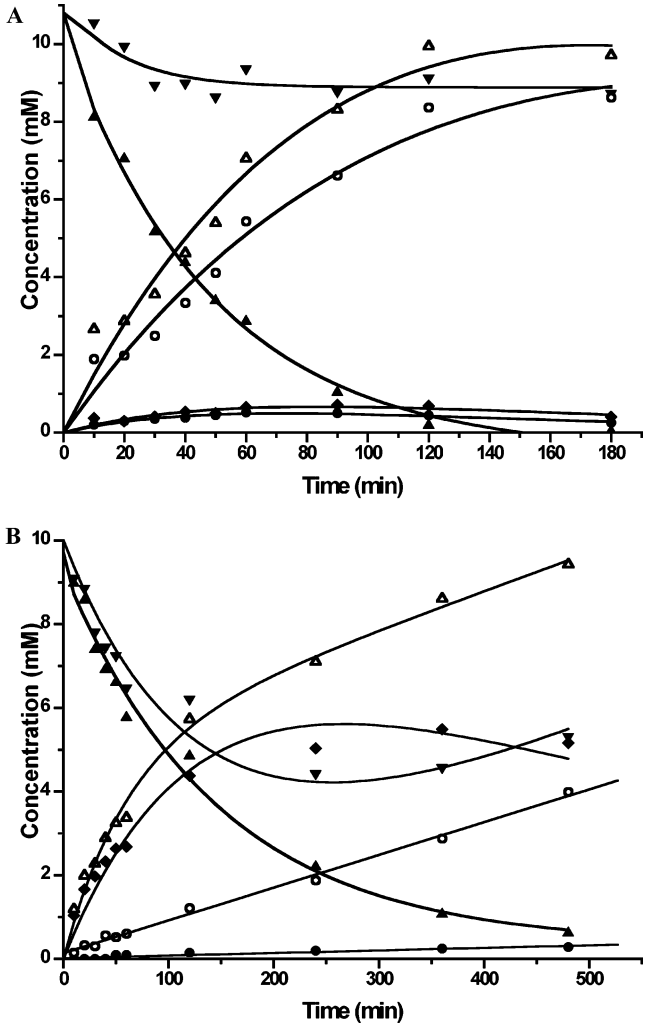

FIGURE 1: Time course of substrate consumption and product formation in the presence of WT Tmαfuc (A) and the C67 mutant (B) with *p*NP-αFuc (10 mM) and *p*NP-*β*Gal (10 mM) as substrates in 50 mM sodium citrate and phosphate buffer and 145 mM NaCl, pH 5 at 40 °C. Key: *p*NP-αFuc (▲), *p*NP-*β*Gal (▼), *p*NP α-L-Fuc*p*-(1→2)-*β*-D-Gal*p* (◆), *p*NP α-L-Fuc*p*-(1→3)-α-L-Fuc*p* (●), fucose (○), and *p*NP (△).

mutations, T264A, Y267F, and L322P, identified after the first round of error-prone PCR on mutants B12, B36, and B3, clearly enhanced the transglycosylation reaction (Table 4). This positive effect was shown to be cumulative with respect to the T/H ratio when these mutations were combined two by two; mutant C67 (T264A/L322P) had better transglycosylation properties than B3 (R147G/L322P) and B12 (T264A), mutant R8 (*M210V*/Y237H/T264A/Y267F) had better transglycosylation properties than B12 (T264A) and B36 (P196L/Y237H/Y267F), and mutant M3 (Y237H/Y267F/L322P) had better transglycosylation properties than B3 (R147G/L322P) and B36 (P196L/Y237H/Y267F). However, when these three identified positive mutations were combined in the same mutants (S1, C2, D2), a dramatic decrease in the overall activity was observed (Tables 3 and 4) while the high transglycosylation to hydrolysis activity ratio (T/H) was retained. It is particularly interesting to notice that all of these beneficial mutations had no direct interaction with substrate or product within the active site.

Synthetic Performance of the Evolved Tmαfuc Mutants. An improvement in the initial T/H activity ratio of glycosidases was a prerequisite for obtaining mutants with good

Table 4: Transglycosylation and Hydrolysis Activities of WT and Mutant Tmαfuc Enzymes in the Presence of *p*NP-αFuc (10 mM) and *p*NP-*β*Gal (10 mM)[a]

	transglycosylation[b] [μ**mol**/(min·mg)]					maximum yield[f] (%)	
mutant	*p*NP Fuc(1→3)Fuc	*p*NP Fuc(1→**2**)Gal	hydrolysis[c] [μ**mol**/(min·mg)]	overall activity[d] [μ**mol**/(min·mg)]	$V_{tran}s/V_{hyd}$[e]	*p*NP Fuc(1→**3**)Fuc	*p*NP Fuc(1→**2**)Gal
WT	198 ± 19	303 ± 110[g]	2954 ± 213	3523 ± 198	0.2	10.3	7
B3	445 ± 41	2612 ± 67[g]	1897 ± 60	5031 ± 73	1.7	12.4	41
B12	568 ± 42	3923 ± 210[g]	1855 ± 230	6603 ± 173	2.6	13.7	42
B36	792 ± 141	2560 ± 191[g]	2694 ± 344	6823 ± 190	1.5	16.9	28
C67	35 ± 7	1545 ± 135	392 ± 100	2010 ± 200	4.0	5.6	55
M3	300 ± 71	3238 ± 288[g]	868 ± 17	4560 ± 364	4.1	6.1	56
N16	622 ± 109	4350 ± 184	2495 ± 67	7467 ± 345	2.0	9.5	40
R8	146 ± 20	2743 ± 148	1330 ± 96	4287 ± 224	2.2	7.2	44
P25	26 ± 3	1650 ± 160	246 ± 32	2020 ± 140	6.8	5.4	62
S1	3.1 ± 0.2	351 ± 21	56 ± 10	401 ± 22	6.3	4.2	55
C2	1.3 ± 0.1	161 ± 4	29 ± 5	189 ± 2	5.5	4.6	59
D2	1.3 ± 0.2	144 ± 24	33 ± 11	177 ± 6	4.4	5.8	65

[a] The activities represent the initial velocities and were measured at 40 °C and pH 5 using purified enzymes. [b] Transglycosylation activity was determined by separation of transglycosylation products by capillary electrophoresis. [c] Hydrolytic activity was calculated by subtracting the transglycosylation activity from the overall activity. [d] The overall activity was determined by the amount of *p*NP released from *p*NP-αFuc. [e] Transglycosylation/hydrolysis ratios were calculated from the initial rates of formation of all transglycosylation products over the initial rate of hydrolysis. [f] Maximum yield corresponds to the transient maximum amount of transglycosylation product obtained after long-term incubation. [g] An additional *p*NP Fuc-Gal regioisomer is formed with this mutant.

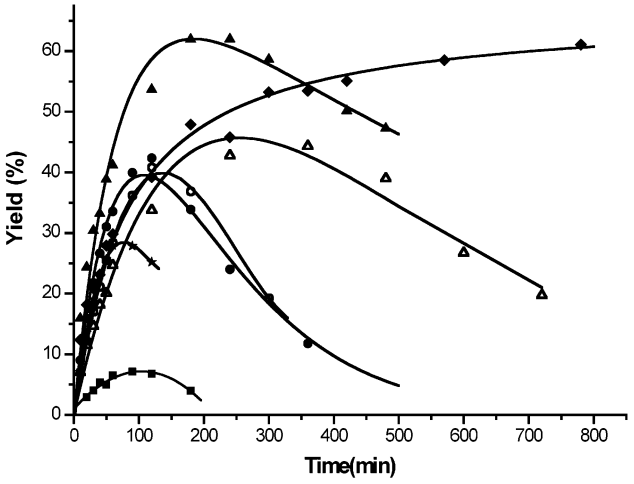

FIGURE 2: Time course of the formation of *p*NP α-L-Fuc*p*-(1→2)-*β*-D-Gal*p* by transglycosylation catalyzed by WT TmαFuc and evolved mutants. The enzyme reaction was performed with *p*NP-αFuc (10 mM), *p*NP-*β*Gal (10 mM), and fucosidases in 600 μL of 50 mM sodium citrate and phosphate buffer and 145 mM NaCl, pH 5 at 40 °C. The yield of *p*NP α-L-Fuc*p*-(1→2)-*β*-D-Gal*p* was determined by capillary electrophoresis. Key: WT Tmαfuc (■), B3 (○), B12 (●), B36 (★), R8 (△), P25 (▲), and D2 (◆).

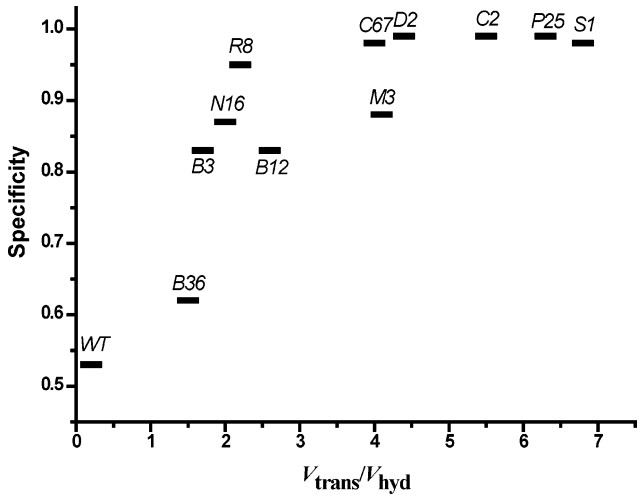

FIGURE 3: Two-dimensional representation of the evolution process of WT Tmαfuc into mutants with high transglycosylation activity. The horizontal axis corresponds to the evolution of the transglycosylation/hydrolysis activity ratio measured at initial rate. The vertical axis represents the specificity of the transglycosylation reaction calculated as the ratio of *p*NP α-L-Fuc*p*-(1→2)-*β*-D-Gal*p* formed to the total concentration of all transglycosylation products at maximum yield.

synthetic capability. However, because the transglycosylation products were kinetic products, the transglycosylation yield was also affected by the rate of hydrolysis of the product, which should be as low as possible to allow accumulation of the transglycosylation products.

Thus, the progress of the transglycosylation products synthesized by evolved Tmαfuc mutants was followed by capillary electrophoresis until nearly complete consumption of substrate (Figures 1 and 2). With WT Tmαfuc, a rapid hydrolysis of the transglycosylation products was observed preventing their accumulation (Figure 1A). A maximum yield of 17% was calculated for transglycosylation products (Table 4). By contrast, evolved mutants like C67 (Figure 1B) exhibited slower substrate (*p*NP-αFuc) and product [*p*NP α-L-Fuc*p*-(1→2)-*β*-D-Gal*p*] hydrolysis, allowing the latter to reach a maximum transient yield of 55%. Figure 2 compares the ability of the Tmαfuc mutants to transfer a fucose residue to *p*NPGal under conditions where the donor/acceptor ratio was 1 (10 mM). These results clearly showed the advantage of the evolved mutants compared to the WT enzyme in relation to their synthetic ability. We progressed from a wild-type enzyme that produced *p*NP α-L-Fuc*p*-(1→2)-*β*-D-Gal*p* at a maximum transient yield of 7% to a recombinant mutant, P25 or D2, which enabled its synthesis at almost 65% yield. Interestingly, this increase in the transglycosylation yield was combined with an increase in the selectivity of the enzyme since, in the most evolved mutants, *p*NP α-L-Fuc*p*-(1→2)-*β*-D-Gal*p* was the major transglycosylation product (>90%). In contrast, the self-condensation product, *p*NP α-L-Fuc*p*-(1→3)-α-L-Fuc*p*, was the major transglycosylation product for the WT enzyme (10%). Figure 3 illustrates the codevelopment of the selectivity and the transglycosylation/hydrolysis activity ratio during the recombination process.

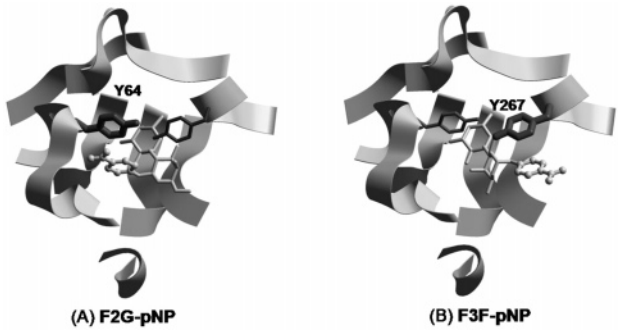

FIGURE 4: Molecular modeling of the transglycosylation products, *p*NP α-L-Fuc*p*-(1→2)-*β*-D-Gal*p* (A) and *p*NP α-L-Fuc*p*-(1→3)-α-L-Fuc*p* (B), within the active site of WT Tmαfuc. Large ribbon segments delimit the catalytic site. Ligands are in thin pale sticks (ball-and-stick representation for the pNP ring). Residues in stacking position with pNP are in thick dark stick representation.

DISCUSSION

We have first demonstrated that the regioselectivity of the fucosyl transfer by WT Tmαfuc and mutants is highly dependent on the sugar acceptor. An α-(1→3) linkage is preferentially formed when the acceptor is *p*NP-fucose, while an α-(1→2) linkage predominates in disaccharides or trisaccharides obtained with *p*NP-Gal and *β*-D-Gal-(1→3)-*β*-D-Glc-O-Ph as acceptors. The OH groups at positions 2 and 3 in both *p*NP-fucose and *p*NP-Gal are, however, in equatorial conformation in their most stable conformation, $^1C_4$ and $^4C_1$, respectively. Thus, they are potentially suitable to form glycosidic linkages with a → e configuration, which was the exclusive linkage formed by most known α-L-fucosidases (*18*). We had anticipated that a possible reason for acceptor-dependent regioselectivity would originate from topological constraints within the binding site. The crystal structure of WT Tmαfuc, which was recently solved (*32*), provided suitable support for molecular modeling calculations in order to understand how a sugar acceptor could affect the transfucosidase regioselectivity. Semirelaxed maps for 1→2, 1→3, and 1→4 product regioisomers yielded four, three, and four possible conformations, respectively. Docking of all possible 1→2, 1→3, and 1→4 regioisomers within the active site revealed that a unique conformation of α-L-Fuc*p*-(1→3)-α-L-Fuc*p* is compatible with the catalytic site topology of the WT. Similarly, only one conformation of *p*NP α-L-Fuc*p*-(1→2)-*β*-D-Gal*p* is preferred inside the catalytic site. However, another conformation of α-L-Fuc*p*-(1→4)-*β*-D-Gal*p* could be possible but with a significantly higher interaction energy (7 kcal/mol more). Interestingly, in the two preferred transfucosylation products, *p*NP α-L-Fuc*p*-(1→3)-α-L-Fuc*p* and *p*NP α-L-Fuc*p*-(1→2)-*β*-D-Gal*p*, the *p*NP moieties point in opposite directions, making a stacking with the phenol group of Tyr267 and Tyr64, respectively (Figure 4). These results emphasize the importance of *p*NP or of an aromatic aglycon part in the binding of acceptors within the +2 binding site of Tmαfuc. Such a preference for sugar substrates having an aromatic substituent has already been observed with most glycosidases (*28*, *38*) and seems to be related to the high density of aromatic residues lining the active site of these enzymes (*32*, *39*, *40*).

Most of the retaining glycosidases, and also fucosidases from the GH29 family, are able to catalyze transglycosylation, but the yields of transglycosylation products are usually low (5−35%) and dependent on the concentration of acceptors (*15*, *18*). Similarly, the wild-type Tmαfuc catalyzed the transfucosylation reactions with low yields (<30%, Table 1) and low specificity, which makes this enzyme unsuitable for synthetic purposes. Because hydrolysis is greatly favored, special conditions have to be used to improve the transfer activity, such as performing the reaction in organic solvent (*20*) or using a high concentration of acceptor (*19*). Furthermore, transglycosylation products obtained with glycosidases are transient species that are subsequently hydrolyzed, a process that also limits the yield of the transglycosylation products. Very high transglycosylation activity is not a common property of these enzymes apart from a few exceptions, such as the trans-sialidase of *Trypanosoma cruzi* (*41*, *42*), cyclodextrin glycosyltransferase (CGTase) (*43*), and glucan sucrases (*44*). The fact that natural evolution has led to enzymes presenting almost exclusive transglycosidase activity suggests that such a property might be accessible by directed molecular evolution of glycosidases. Few examples of the engineering of the hydrolysis/transglycosylation ratio of glycosidase can be found, and most of the results were obtained by site-directed mutagenesis (*45*, *46*). The Withers group (*28*) solved the hydrolysis problem by developing glycosynthases in which the glycosidase catalytic nucleophile is replaced by a nonacidic residue such as alanine. Molecular directed evolution has previously been used to enhance the hydrolytic activity at the expense of the transglycosylation reaction on CGTase (*47*) and by us to improve the transglycosylation activity of *β*-glycosidase from *T. thermophilus* (*26*).

Here, we have shown that it is possible to increase dramatically the transfucosidase activity starting from an α-L-fucosidase by directed evolution. A successful in vitro evolutionary process depends on a screening method that selects the property being searched for. We designed a two-step screening that enables the rejection of mutants with high hydrolytic activity on X-α-fuc, while keeping a high transfer of fucosyl groups to the acceptor *p*NP-*β*Gal. The screening of a relatively small library (5000 clones) provided three mutants (B3, B12, B36) with improved transfer properties, suggesting that structural solutions to improve the transglycosylation activity were not unique. Identification of the positive mutations by preparing single mutants and further rational recombinations have shown that only three mutations have a significant effect on the transfucosylation activity (T264A, Y267F, and L322P). The combination of these mutations, two by two, led to mutants (C67, M3, R8) that retain a higher overall activity than those mutants bearing all three mutations (S1, C2, D2). With these latter mutants, the overall activity was only 5−10% of that of WT enzyme, while mutants M3 and R8 had an overall activity even higher than that of WT enzyme. These results demonstrate that all of these beneficial mutations do not have systematic synergistic effects on the transglycosylation activity and illustrate the limitations of the recombination steps. A possible reason for this nonsynergistic effect is that several evolution pathways can lead to mutants with similar functional phenotypes.

The gain in transglycosidase activity of evolved mutants correlated negatively with the hydrolytic activity. For example, mutant P25, which had the highest transglycosidase/hydrolytic ratio, exhibited a 5-fold increase in transglyco-

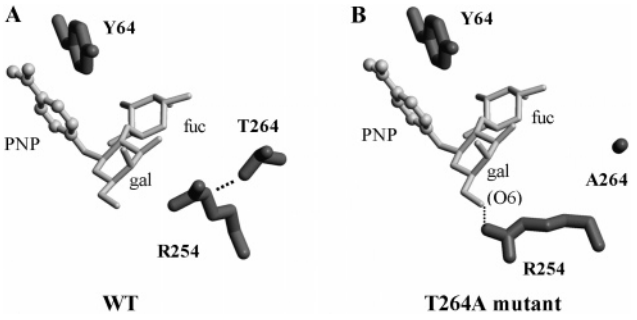

FIGURE 5: Molecular modeling of the effect of the T264A mutation on the structure of Tmαfuc. (A) In the WT enzyme, a hydrogen bond between the guanidinum group of R254 and OH of T264 fixes the orientation of R254 within the active site. (B) In mutant T264A, the R254 side chain would reorient in order to form a new hydrogen bond with the OH-6 of the Gal moiety of the transglycosylation product. (For sake of clarity, only side chains are drawn.)

sylation activity and a 10-fold reduction in hydrolytic activity (Table 4) compared to the WT Tmαfuc. A clear understanding of the reduced hydrolytic activity of the evolved mutants was difficult in the absence of fine structural data for the Michaelis complexes and glycosyl-enzyme intermediates. It has been suggested that the reduced hydrolytic activity observed in *T. cruzi* trans-sialidase could be associated with a greater stabilization of the covalent intermediate, helping to increase the lifetime of the intermediate (*48*). Consistently, the K_m values (Table 3) for *p*NP-αFuc of mutants with low hydrolytic activity were higher than in the WT Tmαfuc. However, k_{cat} values for *p*NP-αFuc did not correlate with the transglycosidase activity since they were dependent on both hydrolytic activity on *p*NP-αFuc and the self-condensation reaction. Some mutants (B3, B12, B36, M3, N16) even exhibited a higher k_{cat} than that of WT Tmαfuc. This surprising result can be partly explained by the inhibitory effect of a high concentration of *p*NP-*β*Gal on the WT enzyme activity. It was shown that *p*NP-*β*Gal and phenyl galactoside acceptors induced a mixed-type inhibition of the wild-type enzyme (data not shown), while mutants were observed to become less sensitive to this inhibition.

Interestingly, all of the beneficial mutations were located in the second shell around the active site and were not in direct contact with the substrates or the products. The crystal structure of WT Tmαfuc (*32*) provides a suitable framework to understand how individual amino acid mutations could affect the transglycosylation activity of mutants. From the 1HL9-B structure, mutated enzymes (L322P, Y267F, and T264A) were built in silico assuming a local and limited geometry perturbation around the mutated residues. Unfortunately, the first two mutations seemed not to comply with this basic assumption (proline residue in the first case and a very flexible loop in the second case). Thus, as suspected, complexes between these mutants and products did not yield a better interaction energy after minimizations, consistent with experimental data. Modeled mutant T264A can explain the transglycosylation efficiency much better. As illustrated in Figure 5, mutation T264A cancelled the hydrogen bond between T264 and R254, inducing a significant reorientation of the R254 side chain in the search for new partners for hydrogen bonding. This is done with the OH-6 of the galactosyl moiety, providing a better docking energy of the product within the binding site. A molecular mechanics scheme gave an interaction energy gain of 7.4 kcal/mol corresponding to at least a supplemental hydrogen bond between the ligand and the modified enzyme (∼3 kcal/mol) in addition to a better fit of the ligand geometry inside the catalytic site. This new hydrogen bond may also explain the increased specificity of the evolved mutants toward the *p*NP-*β*Gal acceptor instead of the *p*NP-αFuc acceptor, OH-6 being absent in this latter substrate. Therefore, the differences in transglycosylation properties seem to arise, at least partly, from amino acid substitutions that indirectly modulate the acceptor binding (*46*). Mutation T264A in the second shell has a direct effect on the side chain reorientation of R254 belonging to the first shell.

The synthesis of carbohydrates with a defined structure remains a challenging goal, and the use of enzymes is an important alternative to chemical synthesis. In this context, the use of glycosyltransferases and their corresponding nucleotide substrate is one possibility but requires an in vitro complex multienzymatic system for nucleotide recycling (*49*). The second possibility is to use retaining glycosidases under special conditions using mutated enzymes (glycosynthase) in which the catalytic nucleophile is replaced by nonnucleophilic residues (*27*−*30*). The glycosynthase strategy has, nevertheless, not yet found universal application, and attempts to develop an α-fucosynthase have not been successful. An additional problem for α-glycosynthase-catalyzed reactions is the instability of the *β*-fluorinated glycoside substrates, particularly if synthesis has to be carried out at elevated temperatures. The other substrate strategy for glycosynthase, using α-fucosides and external nucleophiles such as formate, is hampered by the poor leaving ability of the available fucosyl substrates at low pH (*23*). Then, the third possibility, using modified glycosidases with a high transglycosidase activity, could have a great potential utility in oligosaccharide synthesis. We have shown that it is possible to engineer by directed evolution an α-L-fucosidase that enables synthesis of fucosyl oligosaccharides with high yield (>60%). In some of the best mutants (C2, D2), subsequent hydrolysis of the transglycosylation products is sufficiently slow to allow an efficient recovery of the products without a careful kinetic control of the reaction. In addition, mutants with improved transglycosidase activity are still thermostable enzymes (T_{opt} of 88 °C for most mutants). They retain their activity when stored at room temperature for several months and present good stability in organic solvents such as DMSO (<10%). This property is important for synthesis since solubilization of high concentrations of fucosyl donors requires the addition of such cosolvents. Screening larger mutant libraries for Tmαfuc mutants could provide improved transfucosidases with lower hydrolytic activity, which could be a good alternative for easy access to fucosylated oligosaccharides.

In conclusion, this approach confirms our previous results using a similar strategy on a *β*-D-glycosidase (*26*) and suggests that it could be extended to most retaining glycosidases, even in the absence of precise structural information.

ACKNOWLEDGMENT

We thank B. Freuchet and S. Valéaux for their technical assistance.

REFERENCES

1. Becker, D. J., and Lowe, J. B. (2003) Fucose: biosynthesis and biological function in mammals, *Glycobiology 13*, 41R−53R.

2. Michalski, J. C., and Klein, A. (1999) Glycoprotein lysosomal storage disorders: alpha- and beta-mannosidosis, fucosidosis and alpha-N-acetylgalactosaminidase deficiency, *Biochim. Biophys. Acta 1455*, 69−84.
3. Hakomori, S. (1999) Antigen structure and genetic basis of histo-blood groups A, B and O: their changes associated with human cancer, *Biochim. Biophys. Acta 1473*, 247−266.
4. Imberty, A., Breton, C., Oriol, R., Mollicone, R., and Pérez, S., Eds. (2003) *Biosynthesis, Structure and Conformation of Blood Group Carbohydrate Antigens*, Vol. 2, Elsevier Science B.V., Amsterdam.
5. Le Pendu, J. (2004) Histo-blood group antigen and human milk oligosaccharides. Genetic polymorphism and risk of infectious diseases, *Adv. Exp. Med. Biol. 554*, 135−143.
6. Hutson, A. M., Atmar, R. L., Graham, D. Y., and Estes, M. K. (2002) Norwalk virus infection and disease is associated with ABO histo-blood group type, *J. Infect. Dis. 185*, 1335−1337.
7. Marionneau, S., Ruvoen, N., Le Moullac-Vaidye, B., Clement, M., Cailleau-Thomas, A., Ruiz-Palacois, G., Huang, P., Jiang, X., and Le Pendu, J. (2002) Norwalk virus binds to histo-blood group antigens present on gastroduodenal epithelial cells of secretor individuals, *Gastroenterology 122*, 1967−1977.
8. Ruiz-Palacios, G. M., Cervantes, L. E., Ramos, P., Chavez-Munguia, B., and Newburg, D. S. (2003) *Campylobacter jejuni* binds intestinal H(O) antigen (Fuc alpha 1, 2Gal beta 1, 4GlcNAc), and fucosyloligosaccharides of human milk inhibit its binding and infection, *J. Biol. Chem. 278*, 14112−14120.
9. Holemann, A., and Seeberger, P. H. (2004) Carbohydrate diversity: synthesis of glycoconjugates and complex carbohydrates, *Curr. Opin. Biotechnol. 15*, 615−622.
10. Koeller, K. M., and Wong, C. H. (2000) Complex carbohydrate synthesis tools for glycobiologists: enzyme-based approach and programmable one-pot strategies, *Glycobiology 10*, 1157−1169.
11. Murray, B. W., Takayama, S., Schultz, J., and Wong, C. H. (1996) Mechanism and specificity of human alpha-1,3-fucosyltransferase V, *Biochemistry 35*, 11183−11195.
12. Priem, B., Gilbert, M., Wakarchuk, W. W., Heyraud, A., and Samain, E. (2002) A new fermentation process allows large-scale production of human milk oligosaccharides by metabolically engineered bacteria, *Glycobiology 12*, 235−240.
13. Dumon, C., Samain, E., and Priem, B. (2004) Assessment of the two *Helicobacter pylori* alpha-1,3-fucosyltransferase ortholog genes for the large-scale synthesis of LewisX human milk oligosaccharides by metabolically engineered *Escherichia coli*, *Biotechnol. Prog. 20*, 412−419.
14. Tsuji, Y., Yamamoto, K., and Tochikura, T. (1990) Purification and some properties of a novel alpha-L-fucosidase capable of acting on alpha-(1→6)-L-fucosidic linkages from *Bacillus circulans* M28, *J. Biochem. (Tokyo) 108*, 235−240.
15. Eneyskaya, E. V., Kulminskaya, A. A., Kalkkinen, N., Nifantiev, N. E., Arbatskii, N. P., Saenko, A. I., Chepurnaya, O. V., Arutyunyan, A. V., Shabalin, K. A., and Neustroev, K. N. (2001) An alpha-L-fucosidase from *Thermus* sp. with unusually broad specificity, *Glycoconjugate J. 18*, 827−834.
16. Sano, M., Hayakawa, K., and Kato, I. (1992) Purification and characterization of alpha-L-fucosidase from *Streptomyces* species, *J. Biol. Chem. 267*, 1522−1527.
17. Kobata, A. (1982) alpha-L-fucosidases from almond emulsion, *Methods Enzymol. 83*, 625−631.
18. Berteau, O., Bielicki, J., Kilonda, A., Machy, D., Anson, D. S., and Kenne, L. (2004) Alpha-L-fucosidases: exoglycosidases with unusual transglycosylation properties, *Biochemistry 43*, 7881−7891.
19. Murata, T., Morimoto, S., Zeng, X., Watanabe, S., and Usui, T. (1999) Enzymatic synthesis of alpha-L-fucosyl-N-acetyllactosamines and 3′-O-alpha-L-fucosyllactose utilizing alpha-L-fucosidases, *Carbohydr. Res. 320*, 192−199.
20. Svensson, S. C., and Thiem, J. (1990) Purification of alpha-L-fucosidase by C-glycosylic affinity chromatography, and the enzymic synthesis of alpha-L-fucosyl disaccharides, *Carbohydr. Res. 200*, 391−402.
21. Henrissat, B. (1991) A classification of glycosyl hydrolases based on amino acid sequence similarities, *J. Biochem. 280* (Part 2), 309−316.
22. Tarling, C. A., He, S., Sulzenbacher, G., Bignon, C., Bourne, Y., Henrissat, B., and Withers, S. G. (2003) Identification of the catalytic nucleophile of the family 29 alpha-L-fucosidase from *Thermotoga maritima* through trapping of a covalent glycosyl-enzyme intermediate and mutagenesis, *J. Biol. Chem. 278*, 47394−47399.
23. Cobucci-Ponzano, B., Trincone, A., Giordano, A., Rossi, M., and Moracci, M. (2003) Identification of the catalytic nucleophile of the family 29 alpha-L-fucosidase from *Sulfolobus solfataricus* via chemical rescue of an inactive mutant, *Biochemistry 42*, 9525−9531.
24. Dion, M., Nisole, A., Spangenberg, P., Andre, C., Glottin-Fleury, A., Mattes, R., Tellier, C., and Rabiller, C. (2001) Modulation of the regioselectivity of a *Bacillus* alpha-galactosidase by directed evolution, *Glycoconjugate J. 18*, 215−223.
25. Dion, M., Osanjo, G., Andre, C., Spangenberg, P., Rabiller, C., and Tellier, C. (2001) Identification by saturation mutagenesis of a single residue involved in the alpha-galactosidase AgaB regioselectivity, *Glycoconjugate J. 18*, 457−464.
26. Feng, H. Y., Drone, J., Hoffmann, L., Tran, V., Tellier, C., Rabiller, C., and Dion, M. (2005) Converting a {beta}-glycosidase into a {beta}-transglycosidase by directed evolution, *J. Biol. Chem. 280*, 37088−37097.
27. Drone, J., Feng, H. Y., Tellier, C., Hoffmann, L., Tran, V., Rabiller, C., and Dion, M. (2005) Efficient *Thermus thermophilus* glycosynthases for the synthesis of galactosyl and glucosyl β-(1,3)-glycosides, *Eur. J. Org. Chem.*, 1977−1983.
28. Mackenzie, L. F., Qingping, W., Warren, R. A. J., and Withers, S. G. (1998) Glycosynthases: Mutant glycosidases for oligosaccharide synthesis, *J. Am. Chem. Soc. 120*, 5583−5584.
29. Malet, C., and Planas, A. (1998) From beta-glucanase to beta-glucansynthase: glycosyl transfer to alpha-glycosyl fluorides catalyzed by a mutant endoglucanase lacking its catalytic nucleophile, *FEBS Lett. 440*, 208−212.
30. Okuyama, M., Mori, H., Watanabe, K., Kimura, A., and Chiba, S. (2002) Alpha-glucosidase mutant catalyzes "alpha-glycosynthase"-type reaction, *Biosci., Biotechnol., Biochem. 66*, 928−933.
31. Cobucci-Ponzano, B., Mazzone, M., Rossi, M., and Moracci, M. (2005) Probing the catalytically essential residues of the alpha-L-fucosidase from the hyperthermophilic archaeon *Sulfolobus solfataricus*, *Biochemistry 44*, 6331−6342.
32. Sulzenbacher, G., Bignon, C., Nishimura, T., Tarling, C. A., Withers, S. G., Henrissat, B., and Bourne, Y. (2004) Crystal structure of *Thermotoga maritima* alpha-L-fucosidase. Insights into the catalytic mechanism and the molecular basis for fucosidosis, *J. Biol. Chem. 279*, 13119−13128.
33. Leung, D. W., Chen, E., and Goeddel, D. V. (1989) A method for random mutagenesis of a defined DNA segment using a modified polymerase chain reaction, *Techniques 1*, 11−15.
34. Dinur, U., and Hagler, A. T. (1991) *Review of Computational Chemistry with Discover-InsightII packages of Accelrys* (Lipkowitz, K. B., and Boyd, D. B., Eds.) San Diego, CA, and New York.
35. Andre, G., Buleon, A., Vallee, F., Juy, M., Haser, R., and Tran, V. (1996) Amylose chain behavior in an interacting context. I. Influence of a non-chair ring on the maltose conformation, *Biopolymers 39*, 737−751.
36. Bloom, J. D., Meyer, M. M., Meinhold, P., Otey, C. R., MacMillan, D., and Arnold, F. H. (2005) Evolving strategies for enzyme engineering, *Curr. Opin. Struct. Biol. 15*, 447−452.
37. Kuchner, O., and Arnold, F. H. (1997) Directed evolution of enzyme catalysts, *Trends Biotechnol. 15*, 523−530.
38. Eneyskaya, E. V., Golubev, A. M., Kachurin, A. M., Savel'ev, A. N., and Neustroev, K. N. (1997) Transglycosylation activity of alpha-D-galactosidase from *Trichoderma reesei*. An investigation of the active site, *Carbohydr. Res. 305*, 83−91.
39. Piotukh, K., Serra, V., Borriss, R., and Planas, A. (1999) Protein-carbohydrate interactions defining substrate specificity in *Bacillus* 1,3-1,4-beta-D-glucan 4-glucanohydrolases as dissected by mutational analysis, *Biochemistry 38*, 16092−16104.
40. Marana, S. R. (2006) Molecular basis of substrate specificity in family 1 glycoside hydrolases, *IUBMB Life 58*, 63−73.
41. Buschiazzo, A., Tavares, G. A., Campetella, O., Spinelli, S., Cremona, M. L., Paris, G., Amaya, M. F., Frasch, A. C., and Alzari, P. M. (2000) Structural basis of sialyltransferase activity in trypanosomal sialidases, *EMBO J. 19*, 16−24.
42. Buschiazzo, A., Amaya, M. F., Cremona, M. L., Frasch, A. C., and Alzari, P. M. (2002) The crystal structure and mode of action of trans-sialidase, a key enzyme in *Trypanosoma cruzi* pathogenesis, *Mol. Cell 10*, 757−768.
43. van der Veen, B. A., van Alebeek, G. J., Uitdehaag, J. C., Dijkstra, B. W., and Dijkhuizen, L. (2000) The three transglycosylation

reactions catalyzed by cyclodextrin glycosyltransferase from *Bacillus circulans* (strain 251) proceed via different kinetic mechanisms, *Eur. J. Biochem. 267*, 658−665.

44. Skov, L. K., Mirza, O., Henriksen, A., De Montalk, G. P., Remaud-Simeon, M., Sarcabal, P., Willemot, R. M., Monsan, P., and Gajhede, M. (2001) Amylosucrase, a glucan-synthesizing enzyme from the alpha-amylase family, *J. Biol. Chem. 276*, 25273−25278.
45. Kuroki, R., Weaver, L. H., and Matthews, B. W. (1999) Structural basis of the conversion of T4 lysozyme into a transglycosidase by reengineering the active site, *Proc. Natl. Acad. Sci. U.S.A. 96*, 8949−8954.
46. Paris, G., Ratier, L., Amaya, M. F., Nguyen, T., Alzari, P. M., and Frasch, A. C. (2005) A sialidase mutant displaying trans-sialidase activity, *J. Mol. Biol. 345*, 923−934.
47. Leemhuis, H., Rozeboom, H. J., Wilbrink, M., Euverink, G. J., Dijkstra, B. W., and Dijkhuizen, L. (2003) Conversion of cyclodextrin glycosyltransferase into a starch hydrolase by directed evolution: the role of alanine 230 in acceptor subsite +1, *Biochemistry 42*, 7518−7526.
48. Amaya, M. F., Watts, A. G., Damager, I., Wehenkel, A., Nguyen, T., Buschiazzo, A., Paris, G., Frasch, A. C., Withers, S. G., and Alzari, P. M. (2004) Structural insights into the catalytic mechanism of *Trypanosoma cruzi* trans-sialidase, *Structure 12*, 775−784.
49. Wong, C.-H., Haynie, S. L., and Whitesides, G. M. (1982) Enzyme-catalyzed synthesis on N-acetyllactosamine with in situ regeneration of uridine 5′-diphosphate glucose and uridine 5′-diphosphate galactose, *J. Org. Chem. 47*, 5416.

BI061444W